J. Exp. Biol. (1968), 49, 527–555
With 20 text-figures
Printed in Great Britain

POWER REQUIREMENTS FOR HORIZONTAL FLIGHT IN THE PIGEON *COLUMBA LIVIA*

By C. J. PENNYCUICK
*Department of Zoology, University of Bristol**

(*Received* 24 *April* 1968)

INTRODUCTION

The primary aim of this paper is to estimate the mechanical power required for a pigeon to fly at various speeds. Although this is only one aspect of 'performance' in powered flight, it is perhaps the most informative, and sheds much light on more general performance limitations in flying animals.

Most small and medium-sized flying animals are able to hover, at least for short periods, and they thus share with helicopters the ability to fly horizontally at any speed from zero up to some maximum. Like helicopters, they use the whole lifting surface for propulsion as well as for balancing the weight, instead of using a physically separate source of thrust as in a fixed-wing aeroplane. The more general principles of helicopter theory also apply to flying animals, and are adapted here to investigate the power requirements of the pigeon. Among several excellent textbooks on helicopter engineering, that of Shapiro (1955) has been found especially useful.

The conclusions of the present study are in general agreement with those of Tucker (1968), who made respirometric and other measurements on budgerigars (*Melopsittacus undulatus*) flying in a wind-tunnel. The present power calculation is based entirely on mechanical observations, and provides indirect estimates of such quantities as oxygen consumption, range and endurance, and may thus be regarded as a complementary approach to the same general problem.

MATERIALS AND METHOD

The same pigeons (*Columba livia*) were used as those on which the previous paper (Pennycuick, 1968) was based. Some of the data required in the calculation were derived from the gliding measurements described in that paper, others from further experiments described below, in which the same wind-tunnel and training technique were used. In all the experiments described in this paper the wind-tunnel was set with its axis horizontal, and observations were made with a Bell and Howell 70 DA 16 mm. ciné camera running at 42·6 frames/sec. (determined by filming a clock at the end of each film). Three camera positions were used (Fig. 1): (1) 1·9 m. downstream of the bird, level with the bird and looking upstream; (2) 6·0 m. above the bird, and 1·9 m. downstream; (3) 1·0 m. to one side, looking at right angles to the airstream.

* Present address: Department of Zoology, University College Nairobi, P.O. Box 30197, Nairobi, Kenya.

Additional information was obtained from a film of free-flying pigeons taken on the laboratory roof with a Milliken high-speed camera running at 400 frames/sec. This film was taken by John Hadland (Photographic Instrumentation) Ltd. for the B.B.C., to whom I am most grateful for giving me a copy, and allowing me to use it for research purposes.

HORIZONTAL FLIGHT MEASUREMENTS

Various quantities required in the power calculation were measured as functions of forward speed, as follows:

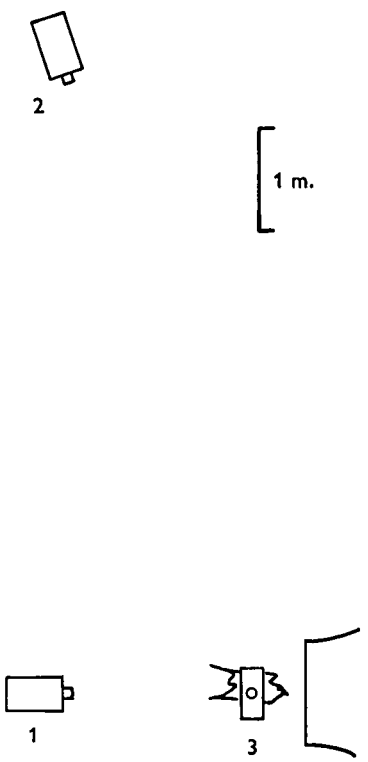

Fig. 1. Ciné camera positions, numbered as in the text.

Sweep angle (σ) *and wingbeat frequency* (F)

Sweep angle is defined as the aggregate angle swept through by the humeri of both wings during the downstroke. It was determined by filming a pigeon in horizontal flight from behind (camera position 1, Fig. 1). The film was later back-projected onto squared paper and examined frame by frame. Figure 2 shows tracings of two frames, at the beginning and end of a downstroke. The angle between the estimated positions of the humeri was measured at each position, and the difference between these angles gives the sweep angle for that stroke. Pigeons did not fly absolutely steadily in the tunnel, and in practice both sweep angle and wingbeat frequency varied periodically, with a tendency for bursts of vigorous flapping every 5–10 wingbeats. The graph of Fig. 3 is based on an average of 30 wingbeats for each point.

Wingbeat frequency was determined simultaneously with sweep angle, by counting frames over a whole number of wingbeats, starting and finishing at the beginning of a downstroke.The results are plotted in Fig. 4.

The points for zero speed in Figs. 3 and 4 are derived from the high-speed film referred to on page 528, which was taken in anticyclonic conditions, with no detectable wind. Two sequences were found, one of 5 and one of 8 wingbeats, in which a pigeon remained approximately stationary, and the wingbeat frequency was 6·9/sec. in both cases. The sweep angle was assumed to be the maximum recorded by Pennycuick & Parker (1966), 284°. The zero-speed points of Figs. 3 and 4 are somewhat more conjectural than the others, because of uncertainty that the birds' airspeed really was zero.

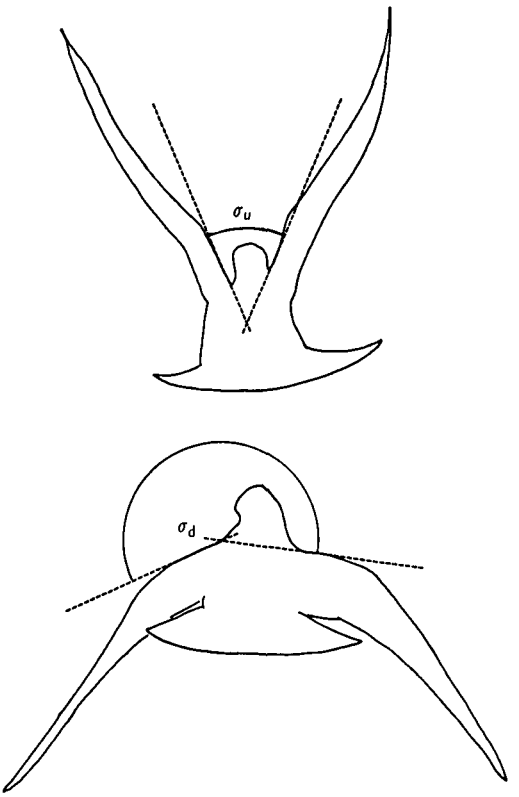

Fig. 2. Tracings of two frames from a film taken from camera position 1 (Fig. 1), showing consecutive fully 'up' and fully 'down' wing positions. 'Sweep angle', σ, for that downstroke is defined as $\sigma = \sigma_d - \sigma_u$.

Inclinication of flapping plane Φ

When a bird hovers it beats its wings back and forth horizontally, and the faster it goes, the more nearly the plane in which the wings beat becomes vertical. The 'inclination of the flapping plane' is defined as zero when the wings beat horizontally, and 90° when they beat vertically. It was measured from a film taken from camera position 3 (Fig. 1), in which the pigeon was photographed against a background con-

sisting of a white card, ruled with black lines parallel to the airflow. The film was back-projected frame by frame onto squared paper, one axis of which was aligned with these lines. The position of the leading edge of the wing at the wrist joint was marked at the beginning and end of the downstroke as shown in Fig. 5, and the acute angle between the airflow and the line joining the two marks was measured. Measurements were made on an average of 20 wingbeats at each speed, in order to minimize errors caused by movement of the pigeon upstream or downstream. The results are plotted in Fig. 6.

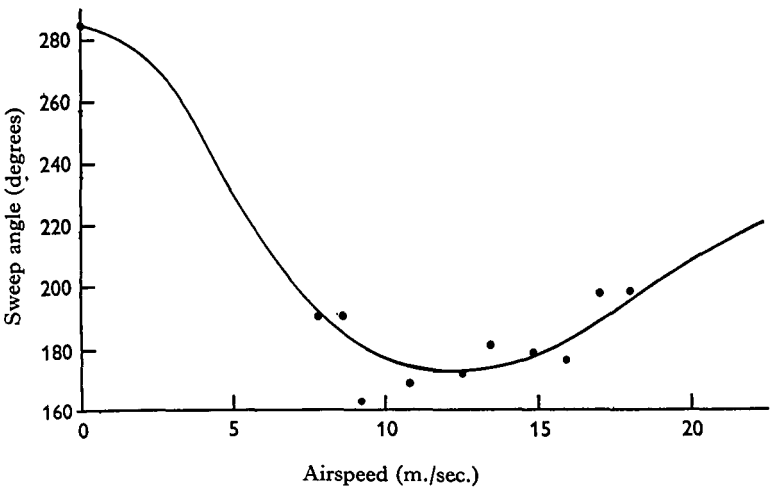

Fig. 3. Measurements of sweep angle at various speeds. The line was drawn in by eye, and was represented in the computer programme by a fourth degree polynomial.

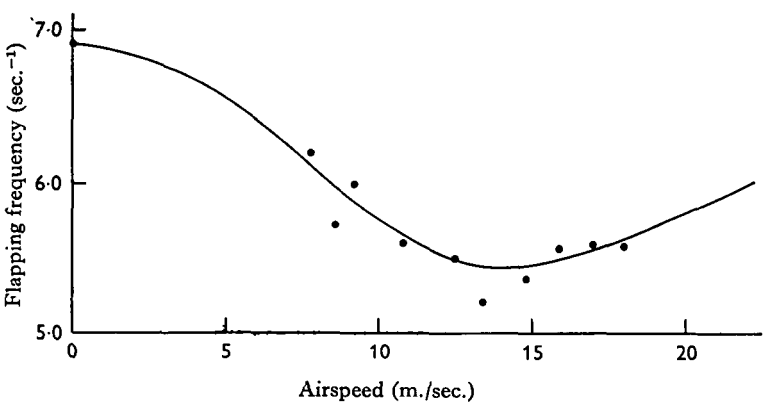

Fig. 4. Flapping frequency versus speed. The significance of the line is as in Fig. 3.

ANALYSIS OF POWER REQUIREMENTS

In horizontal flight at constant speed power is absorbed in three ways: (1) Induced power—the power needed to impart downward momentum to the air, sufficiently rapidly to produce a reaction balancing the bird's weight; (2) profile power—the

power needed to overcome the profile drag of the wing; (3) parasite power—the power needed to overcome the drag of non-lifting parts, i.e. the body in the case of a bird.

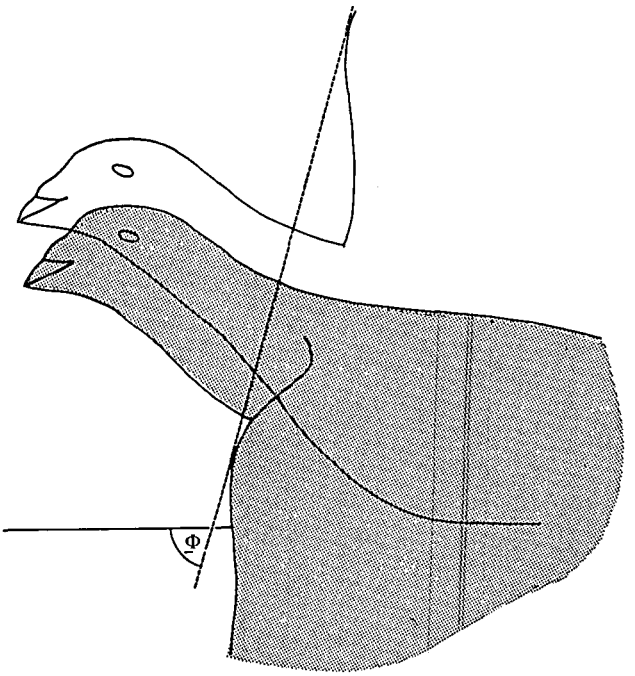

Fig. 5. Tracings of two frames, superimposed, taken from camera position 3 (Fig. 1), showing consecutive fully 'up' and fully 'down' wing positions. The horizontal line, ruled on a card beyond the pigeon, shows the direction of the airflow. The 'inclination of the flapping plane', Φ, is defined as the acute angle between this line and the dotted line.

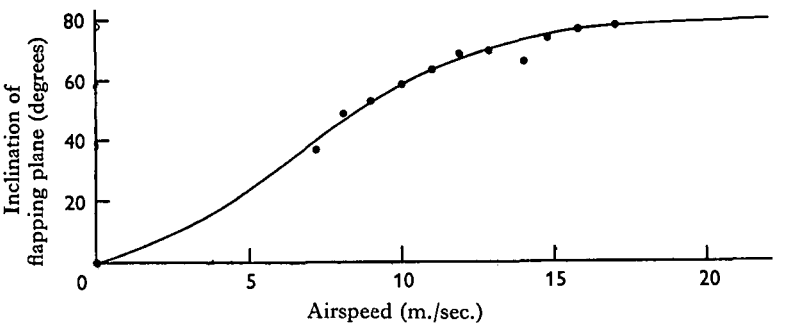

Fig. 6. Inclination of the flapping plane versus speed. The significance of the line is as in Fig. 3.

In non-horizontal flight one must also include *climbing power*, which is equal to the product of the weight, and any upward component of speed. A particular climbing case is considered on page 544.

The power required for a pigeon to fly horizontally at speeds ranging from 0 to 22 m./sec. was estimated with the aid of Bristol University's Elliott 503 computer. The above three components of power were calculated in turn, as follows.

Induced power

In horizontal flight, the upward reaction on the wings must equal the weight, and this implies that the rate at which downward momentum is imparted to the air is numerically equal to the weight. This rate of change of momentum is the product of a downward *induced velocity* and the mass of air to which this velocity is imparted in unit time.

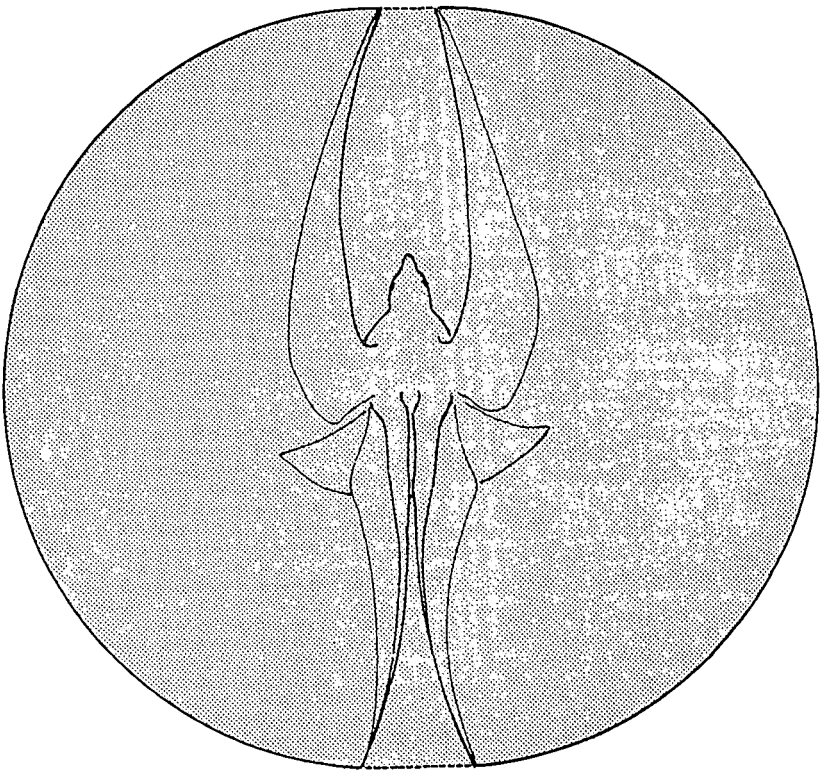

Fig. 7. View of a hovering pigeon from above, the wings beating horizontally. The stippled area is defined as the 'disk area', S_d.

Considering the hovering case first, the bird's body remains stationary and the wings beat horizontally, sweeping out an area (as seen from above) which is referred to as the disk area (S_d) (Fig. 7). The airflow through the wing disk is entirely due to the induced velocity V_{iz}. The following simplifying assumptions, which give good approximations in calculating helicopter performance, are adopted here. (1) The induced velocity is assumed to be constant over the entire disk area. (2) An abrupt pressure rise is assumed to occur as the air passes downward through the disk. This pressure increment, multiplied by the disk area, must, of course, equal the bird's weight. Half of the pressure step is assumed to be contributed by an area of reduced pressure (relative to ambient) above the wing disk, and half by increased pressure below it.

The term 'induced velocity' (V_{iz}) here refers to the velocity with which the air passes through the wing disk, and it reaches this velocity as a result of accelerating

downwards into the area of reduced pressure above the wing disk. Because there is a similar pressure gradient below the bird, the air continues to accelerate downwards after passing through the wing disk, and eventually reaches a velocity of $2V_{iz}$ far below the bird. This is proved in all textbooks on helicopters, and is illustrated diagrammatically in Fig. 8.

The induced velocity in hovering is easily calculated in the basis of the above assumptions. The mass flow (f_m) is the rate at which mass passes through the wing disk, and is given by

$$f_m = S_d V_{iz} \rho, \tag{1}$$

where ρ is the air density.

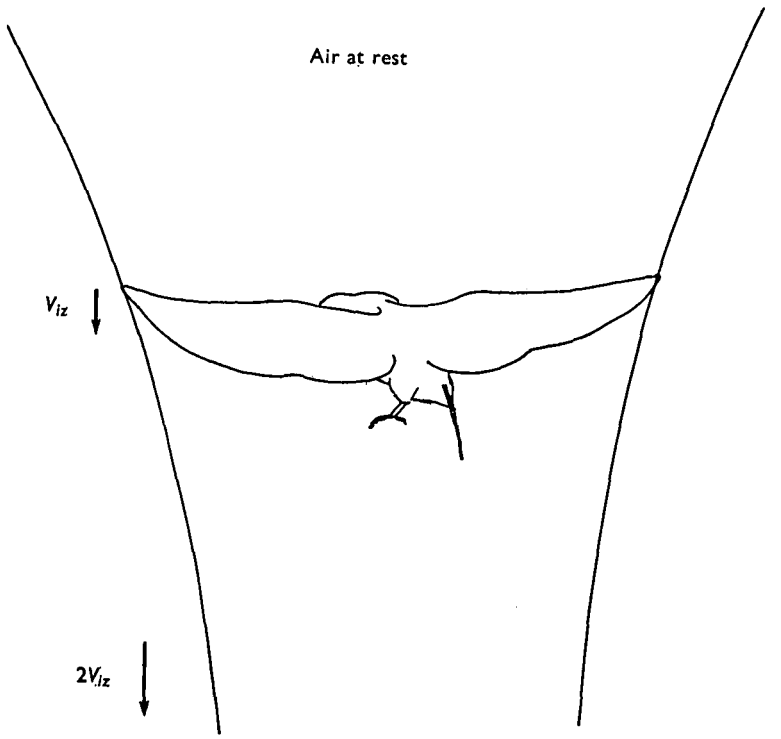

Fig. 8. Airflow past a hovering pigeon, seen from the side. Air is drawn from rest far above the bird, passes downwards through the wing disk at the 'induced velocity' V_{iz}, and eventually accelerates to $2V_{iz}$ far below the bird.

The air is eventually accelerated to $2V_{iz}$, and so the rate of change of momentum, which equals the weight W, is

$$2f_m V_{iz} = W = 2S_d V_{iz}^2 \rho, \tag{2}$$

so that

$$V_{iz} = \sqrt{\left(\frac{W}{S_d}\frac{1}{2\rho}\right)}. \tag{3}$$

The induced velocity is thus proportional to the square root of the *disk loading*, which is defined as the ratio (W/S_d). The induced power P_i is

$$P_i = WV_{iz} = W\sqrt{\left(\frac{W}{S_d}\frac{1}{2\rho}\right)}. \tag{4}$$

In forward flight the weight must still be balanced by the rate of change of downward momentum imparted to the air. The mass flow through the wing disk is now, however, the product of the density, the disk area, and the resultant of the induced velocity and the forward speed. The faster the bird goes, the more mass passes through the wing disk in unit time, and the less induced velocity is needed to produce the requisite rate of change of momentum. At a forward speed V the mass flow is

$$f_m = \rho S_d \sqrt{(V^2 + V_{iz}^2)}, \tag{5}$$

so that the rate of change of momentum is

$$2V_{iz} f_m = W = 2\rho S_d V_{iz} \sqrt{(V^2 + V_{iz}^2)}. \tag{6}$$

The induced power is still the product of the weight and the induced velocity, so that

$$P_i = WV_{iz} = 2\rho S_d V_{iz}^2 \sqrt{(V^2 + V_{iz}^2)}. \tag{7}$$

Validity of constant disk area

In view of the finding in the previous paper (Pennycuick, 1968) that wing-span in gliding flight is progressively reduced with increasing speed, it might be wondered whether the same is true in horizontal flapping flight, and a film was taken from above (camera position 2 in Fig. 1) in order to check this point. It was found that the wings were extended to their full span on the downstroke at all speeds at which the pigeon would fly horizontally. On the upstroke, however, span was reduced at high speeds in roughly the same way as in gliding. In fast flight the pigeon extends its wings fully at the start of the downstroke, and at the bottom of the downstroke it flexes the carpal joints, and keeps them flexed during the upstroke. The alternate flexion and extension of the carpal joints is clearly seen in the high-speed film of free-flying pigeons.

The fact that the wings only sweep through some 170° out of the full 360° of the disk at medium speeds is of no account. For the purpose of calculating mass flow, 'disk area' remains the full circle, whose diameter is equal to the wing-span, whether the wings are flapped or not. The induced velocity for a fixed-wing aeroplane or glider is calculated by considering the mass flow through a circle, whose diameter is equal to the wing-span.

Horizontal induced power

In forward flight the drag of the body has to be overcome by imparting *backward* momentum to the air, and this horizontal component of induced velocity can be calculated in basically the same way as the vertical component. The horizontal induced velocity increases progressively with speed, and amounts to about 0·1 % of the forward speed. The power needed to generate it would not reach 0·02 W. over the speed range considered, and can be neglected. For similar reasons as apply in the case of vertical induced power, the induced power needed to overcome a given drag is inversely proportional to the square root of the disk area. Thus much less induced power is needed to overcome body drag if the whole wing is flapped than if the thrust is derived from a propeller or jet, whose diameter is much smaller than the wing span.

Profile power

The calculation of profile power is somewhat laborious, and could not have been undertaken without using the computer. The difficulty is that the speed and direction of the relative airflow is different at every point along a flapping wing, so that the behaviour of the whole wing has to be approximated by some form of strip analysis. The following calculation refers only to the downstroke, profile power on the upstroke being estimated separately on page 538.

The outline of one wing of the pigeon on whom most of the wind-tunnel measurements were made was traced on graph paper, and the tracing was divided span-wise into thirty-two strips, each 1 cm. wide. The areas of these strips were measured, S_i

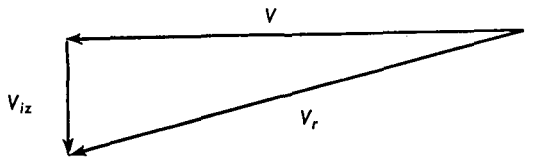

Fig. 9. Triangle of velocities showing the forward speed V, the induced velocity V_{iz} and their resultant V_r.

being the area of strip i (see appendix). Each strip was assigned a flapping radius, that is, the distance of its assumed centre of lift from the centre of rotation of the head of the humerus. The arrangement of strips was such that the flapping radius r_i of strip i was i cm.

V_{iz} was first calculated (see p. 534), and hence the magnitude of the resultant velocity V_r (Fig. 9) where

$$V_r = \sqrt{(V_{iz}^2 + V^2)}. \tag{8}$$

The downwash angle ϵ is given by

$$\epsilon = \tan^{-1}\left(\frac{V_{iz}}{V}\right). \tag{9}$$

This defines the general flow, whose magnitude and velocity is the same for the whole wing. It now has to be combined with a flapping velocity V_{fi} which is different for each strip. Its magnitude at strip i is given by

$$V_{fi} = \omega r_i, \tag{10}$$

where ω is the angular velocity of the wing during the downstroke. It is the angle swept through by one wing in a downstroke, divided by half the period of one complete wingbeat cycle, and is thus equal to the product of sweep angle (for both wings, as defined on page 528) and flapping frequency.

Figure 10 shows V_r and V_{fi}, and their resultant V_{ri}, which is the local resultant velocity at strip i. V_{ri} is inclined at an angle B_i to the horizontal. It can be seen from Fig. 10 that

$$V_{ri} = \sqrt{[V_r^2 + V_{fi}^2 - 2V_rV_{fi}\cos(\pi - \Phi - \epsilon)]} \tag{11}$$

and

$$B_i = \sin^{-1}\left[\frac{V_{fi}\sin(\pi - \Phi - \epsilon)}{V_{ri}}\right] - \epsilon. \tag{12}$$

The force F_i in Fig. 10 is the resultant of the local lift L_i and the profile drag D_{pi} on strip i. It is inclined at an angle ϕ_i to the vertical, where

$$\phi_i = \tfrac{1}{2}\pi - B_i - \Psi. \tag{13}$$

Ψ, which is assumed to be the same for all strips, is given by

$$\Psi = \tan^{-1}\left(\frac{L_i}{D_{pi}}\right). \tag{14}$$

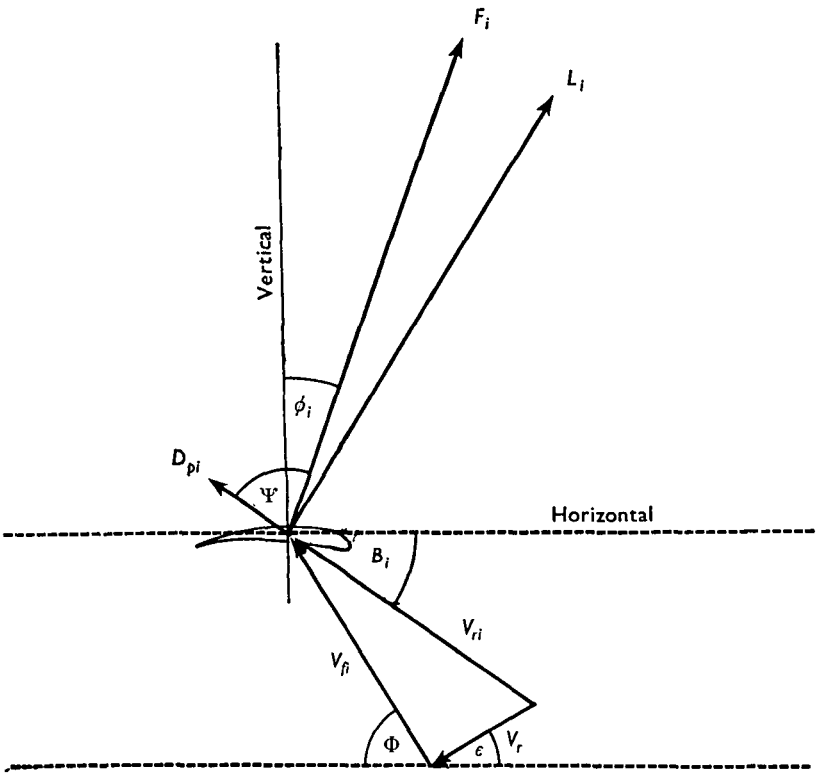

Fig. 10. Local velocities and forces at strip i of the wing in horizontal flapping flight. V_{ri} is the resultant of V_r (see Fig. 9) and the local flapping velocity V_{fi}. L_i and D_{pi} are the lift and profile drag respectively, and F_i is their resultant.

Evidently strip i contributes a vertical component of force $F_i \cos \phi_i$ towards balancing the bird's weight W, so that for one wing divided into n strips

$$\sum_{i=1}^{i=n} F_i \cos \phi_i = \tfrac{1}{2}W. \tag{15}$$

The force F_i is different for each strip, but can be represented by a dimensionless coefficient C_F which can, with reasonable plausibility, be assumed to be the same for the whole wing:

$$C_F = \frac{F_i}{\tfrac{1}{2}\rho V_{ri}^2 S_i}. \tag{16}$$

From equations (15) and (16)

$$\tfrac{1}{2}W = \tfrac{1}{2}\rho C_F \sum_{i=1}^{i=n} V_{ri}^2 S_i \cos \phi_i$$

so that

$$C_F = \frac{W}{\rho \sum_{i=1}^{i=n} V_{ri}^2 S_i \cos \phi_i}. \tag{17}$$

C_F is the resultant of the lift coefficient C_L and the profile drag coefficient C_{DO}. If the ratio of these coefficients (or the angle Ψ) is known, C_L can be obtained from C_F by the relation

$$C_L = C_F \sin \Psi. \tag{18}$$

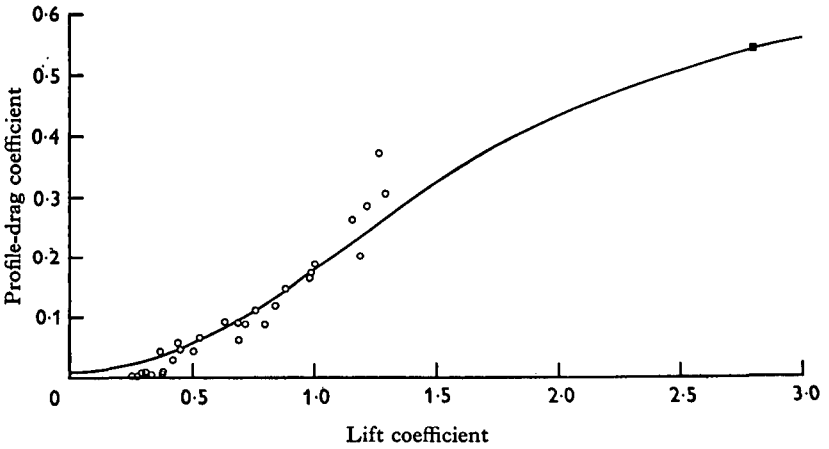

Fig. 11. Profile drag coefficient as a function of lift coefficient, measured in gliding flight (Pennycuick, 196). The line is drawn in by eye to give a minimum C_{DO} of 0·01, and extrapolated to cover the highest lift coefficient required in flapping flight (black square). It was fitted by a fourth-degree polynomial to enable profile drag coefficient to be calculated in the computer program.

Unfortunately Ψ cannot be estimated until C_L is known, and had to be found in the program by iteration. A trial value of $\Psi = 1{\cdot}5$ radians was first used, and on this basis ϕ_i was calculated for each strip from equation (13), and thence C_L from equations (17) and (18). C_{DO} was now calculated from the curve of Fig. 11, which was derived from the gliding measurements described in the previous paper, and represented in the program by a fourth-degree polynomial. The validity of this step is considered on page 539. A new value of Ψ was now obtained from the relation

$$\Psi = \tan^{-1} \frac{C_L}{C_{DO}}, \tag{14}$$

and this was used to calculate a new set of values for ϕ_i, and hence new values for C_L and C_{DO}. This was repeated until the value of Ψ changed less than 0·001 radian in successive repetitions of the cycle.

Having found a value for C_{DO} which is assumed to apply to the whole wing, the profile drag of each strip can now be calculated, and hence the power needed to overcome the profile drag of the whole wing. This profile power may conveniently be

divided into two components: P_{pro1} is the power needed to maintain the wing's angular velocity in the downstroke, while P_{pro2} is that needed to overcome that component of the profile drag which opposes the forward movement of the whole bird.

(*a*) P_{pro1}

The profile drag on strip i acts parallel to the local relative airflow, but in general not parallel to the flapping direction (Fig. 10). The angle θ_i between the local relative airflow and the flapping direction is

$$\theta_i = \Phi - B. \tag{19}$$

The work Q_i done against the profile drag of strip i, by rotating the wing through one downstroke, is therefore

$$Q_i = D_{pi} \cos \theta_i \tfrac{1}{2} \sigma r_i, \tag{20}$$

so that for all the strips of both wings the power required is

$$P_{pro1} = \sigma F \sum_{i=1}^{i=n} D_{pi} r_i \cos \theta_i. \tag{21}$$

(*b*) P_{pro2}

The component of the profile drag on strip i acting parallel to the flight direction is $D_{pi} \cos B_i$ (Fig. 10). The power needed to overcome it is the product of this component of drag and the forward speed, so that for the whole of one wing

$$P_{pro2} = V \sum_{i=1}^{i=n} D_{pi} \cos B_i. \tag{22}$$

This needs to be doubled to cover both wings, but, as only the downstroke is being considered at present, only half the cycle is involved—thus equation (22) can be used as it stands to represent P_{pro2} for both wings, for the downstroke only.

Profile power in the upstroke

In fast flight the wing could well be elevated passively; it is difficult to estimate the work done (if any) by the flight muscles during such elevation, but this would certainly be small, and is neglected. Some power must, however, be needed to counteract the retarding effect of wing profile drag on the forward motion of the bird, and to allow for this P_{pro2} is doubled. This may be pessimistic, since wing-span and area are reduced during the upstroke in fast horizontal flight, which should produce a reduction of wing profile drag (Pennycuick, 1968). Any such saving is difficult to estimate, however, and at present doubling P_{pro2} is the best method available for allowing for wing profile drag during the upstroke. It is assumed, in effect, that P_{pro1} is present during the downstroke only, whereas P_{pro2} continues throughout both the downstroke and the upstroke.

At very low speeds elevation of the wing is certainly active (Brown, 1948), and some work is done, presumably by the supracoracoideus. Pennycuick & Parker (1966) estimated that the maximum work done in one contraction by the supracoracoideus would be 8·5% of that done by the pectoralis, and on this basis one could suggest that the supracoracoideus should contribute about 0·26 W. to the profile power during hovering, when this component is presumably maximal. This is conjectural, however, and, as this component appears to be small, it too is neglected.

Simplifications in profile drag calculation

(1) *Direction of forces.* Strictly speaking, the profile power calculation refers only to the mid-point of the downstroke, except in hovering, where the wingbeat plane is horizontal. At low speeds, where the wingbeat plane is nearly horizontal, the error from this source would be small, whereas at higher speeds the sweep angle is reduced and the wing can be assumed to do most of its work within $\pm 30°$ of the horizontal position. This complication has therefore been neglected.

(2) *Calculation of profile-drag coefficient.* The relation between C_{DO} and C_L (Fig. 11) is based on the gliding measurements of the preceding paper (Pennycuick, 1968), where the observations at high C_L refer to the fully extended wing, while those at low C_L refer to the wing with carpal joint flexed. It was not possible to test the extended wing at low lift coefficients. In horizontal flight the wing is extended during the downstroke at all speeds, and it is possible that at high speeds the estimated profile-drag coefficient is in error because of this.

At very low speeds the lift coefficient far exceeds the maximum obtainable in gliding pigeons, so that one has to guess at the profile-drag coefficient. The curve has been extrapolated on the assumption that at a lift coefficient of 2·8 a profile drag coefficient of 0·54 would prevail, which it is hoped is a sufficiently pessimistic assumption. The left-hand end of the curve has also been adjusted; it was explained in the preceding paper (Pennycuick, 1968) that the very low values of wing profile drag obtained at high gliding speeds are subject to some doubt, so in order to avoid the risk of undue optimism the curve was made to give a minimum C_{DO} of 0·01, ignoring the lowest experimental points which are in the region of 0·003.

It can be seen that because of these various reservations the estimated profile power is subject to rather more doubt than the other two components.

Parasite power

Parasite power P_{par} is that needed to overcome the drag of the body, and is given by

$$P_{\text{par}} = \tfrac{1}{2}\rho V_r^3 S_p C_{Dp}, \tag{23}$$

where S_p is the frontal area of the body and C_{Dp} is its drag coefficient.

From the results of the preceding paper C_{Dp} was taken to be 0·43 and S_p was taken to be 36 cm.^{2}—that is, the body was taken to be equivalent to a flat plate 15·5 cm.^{2} in area. It may be noted in passing that this constitutes a parasite-drag ratio of 0·0044; that is, the ratio of the equivalent flat plate area of the body to the disk area. This would be considered a medium value of parasite-drag ratio in helicopter practice (Shapiro, 1955).

The power-versus-speed curve

The three calculated components of power are plotted against speed in Fig. 12. Induced power is 8·4 W. in hovering, but declines rapidly as speed is increased, and falls below 2 W. at speeds above 9 m./sec. Parasite power, on the other hand, is negligible at low speeds, and remains below 1 W. up to 10 m./sec., after which it increases rapidly to become the largest component above 19 m./sec. Profile power is roughly constant between 5 and 6 W. over the range 3–18 m./sec., and is the largest component over most of the speed range, from about 4 to 19 m./sec.

Although the power calculation contains many assumptions and approximations, the more important of which have (it is hoped) been pointed out, there is no reason to doubt that the main trends are as shown in Fig. 12—that is, the induced power is high in hovering and drops sharply with increasing speed, the parasite power starts at zero, and increases with roughly the cube of the speed, and the profile power is substantial at all speeds.

The sum of the three components is the total power required to fly at any particular speed, and this is also plotted against speed in Fig. 12. The calculated total power is about 11·5 W. in hovering but declines steeply as speed is increased to a minimum of 8·7 W. at 8–9 m./sec. Above this speed the total power again rises. The slight hump in the curve of Fig. 12 at about 1 m./sec. results from the very high drag coefficient assumed to prevail at low speeds, and should not be taken too literally.

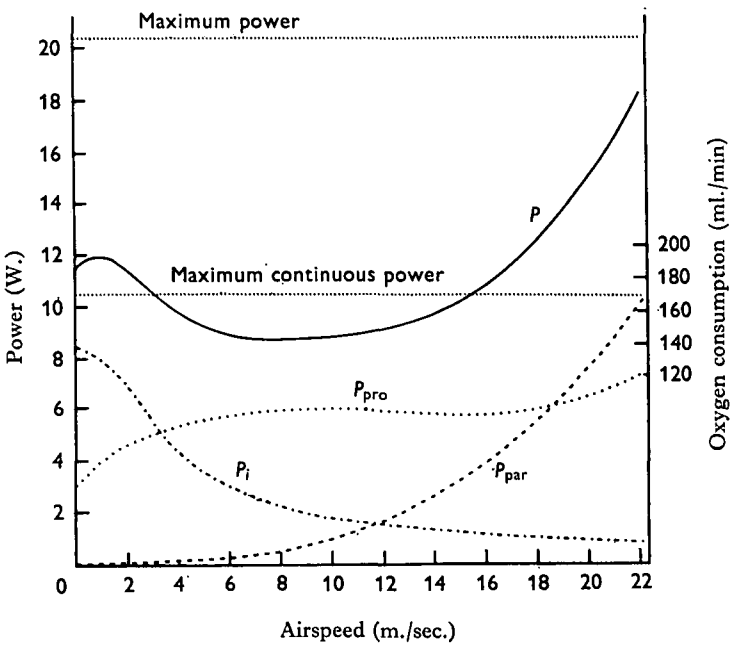

Fig. 12. Calculated power required and power available plotted against speed for the pigeon (see text). The corresponding oxygen consumption is shown at right. P_i, Induced power; P_{pro}, profile power; P_{par}, parasite power; P, total power.

The *minimum-power speed*, about 8–9 m./sec., is about the same as the minimum gliding speed (about 8·6 m./sec.), and the power required to fly at this speed is only about three-quarters of that required in hovering. It is the speed at which the bird should fly if its object is to remain airborne for as long as possible on a given amount of fuel—but not if it needs to travel the maximum possible distance for a given amount of fuel.

Range

If P is the power in watts, and V the forward speed in m./sec. then the ratio

$$E = \frac{V}{P} \tag{24}$$

is the distance in metres travelled per joule of work done. To gain an idea of the pigeon's fuel consumption, it will be assumed that oxidation of 1 g. of fat yields 40,000 joules of energy, and that 20% of this, or 8000 J. is available as mechanical work. The distance in kilometres, flown per gram of fat oxidized, calculated on this basis, is plotted against speed in Fig. 13. The maximum, 11·8 km./g., is achieved at 16 m./sec.: this *maximum-range speed* is much faster than the minimum power speed (8–9 m./sec.), at which only about 8 km. would be flown per gram of fat oxidized.

To assess a pigeon's effective range, a large (471 g.) male pigeon was killed, and the total fat was extracted with hot chloroform in a Soxhlet apparatus; 37·4 g. of fat were extracted. If the pigeon were to oxidize the whole of this by flying at its maximum-range speed of 16 m./sec., it would travel about 400 air km., and be airborne for about 7 hr. The pigeon used for this estimate had been kept on a ration of 28 g. of mixed seed per day, which would be normal for racing pigeons flying on medium-distance races of 300 km. or so. A fat pigeon would probably contain at least twice as much fat as the one extracted. Exceptionally good racing pigeons do on occasion home over distances as great as 800 km. in a single summer's day, with perhaps 15 hr. flying time. On the basis of the above calculation, this would call for a usable fat store of some 70 g., which would appear quite feasible.

Effective lift:drag ratio

In a fixed-wing aircraft flying horizontally at a constant speed V the weight W is balanced by the lift L provided by the wings, and the drag D is balanced by the thrust T of the propeller or jet (Fig. 14). The power required, P, is then

$$P = TV = DV = WV\frac{D}{L}. \tag{25}$$

If the power, weight and speed are known, the lift:drag ratio is given by

$$\frac{L}{D} = \frac{WV}{P}. \tag{26}$$

In the same way an *effective lift:drag ratio* can be defined for a helicopter or a bird in horizontal flight as

$$\left(\frac{L}{D}\right)_{\text{eff}} = \frac{WV}{P}. \tag{26}$$

Although this quantity has not the simple physical meaning indicated by Fig. 14 for a fixed-wing aircraft, it has a similar significance in performance analysis. It is a dimensionless number which can be used to compare the aerodynamic efficiency of flying machines or animals of different sizes and weights.

The effective lift:drag ratio, when divided by the weight, yields the distance flown per unit work done (equation 24). Thus if E is the mass of fuel carried (expressed in energy units), the range R is given by

$$R = \left(\frac{L}{D}\right)_{\text{eff}} \frac{E}{W}. \tag{27}$$

To a first approximation the amount of fuel carried is likely to be a fixed proportion of the take-off weight in animals or aircraft of different size. In this case range is

proportional to lift:drag ratio only, and is independent of weight, since the ratio E/W is constant. It need cause no surprise to learn that a ruby-throated hummingbird (*Archilochus colubris*) can fly the 500 miles across the Gulf of Mexico non-stop (Lasiewski, 1962). The feat is not inherently more difficult for a small bird than for a large one, and implies only that the hummingbird has as good an effective lift:drag ratio as larger birds (see also p. 547).

The curve of $(L/D)_{eff}$ versus speed for the pigeon has the same form as the range curve of Fig. 13, and is shown on the same graph. Its maximum value is estimated to be 5·9. This is a poor value by helicopter standards, where values of $(L/D)_{eff}$ of 15 are commonly obtained, and 20 is not unknown. The poor estimated performance for the pigeon is partly due to the high wing profile coefficients assumed, and partly to the large equivalent flat plate area of the body. Both quantities are derived from gliding measurements, and there are no grounds at present for regarding them as pessimistic.

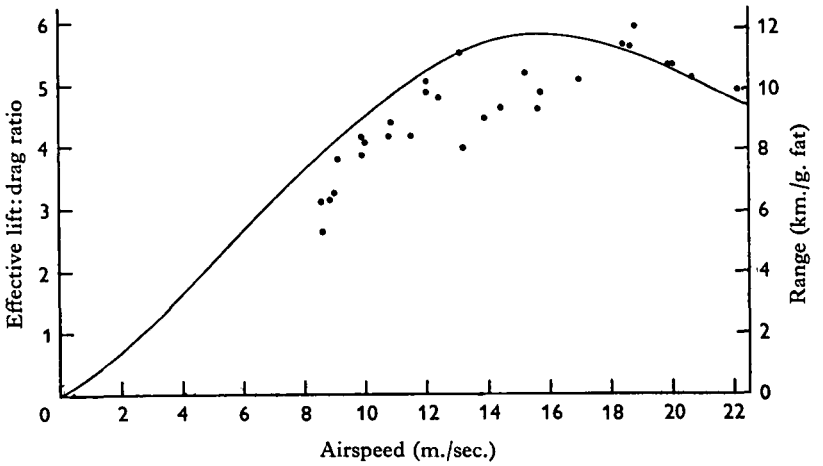

Fig. 13. Calculated effective lift:drag ratio, and range per gram of fat oxidized, plotted against speed for the pigeon.

An estimate of effective lift:drag ratio for a smaller bird, the blackpoll warbler *Dendroica striata*, can be obtained from figures given by Nisbet, Drury & Baird (1963) for fat consumption during long migratory flights over the sea. By comparing the fat stores of samples of birds taken before and after a sea crossing, they estimated that these birds, whose average weight was 19·0 g. wt., used 1·02 kcal. of chemical energy per hour. If one-fifth of this is assumed to have been converted into mechanical work, the average power output would be 854 J./hr. The birds are stated to fly at about 20 knots (37 km./hr.). Substituting these figures in equation (26) yields an effective lift:drag ratio of 8·1. When it is remembered that the figure given by Nisbet *et al.* (1963) for fat consumption represents a minimal estimate, so that the resulting estimate of $(L/D)_{eff}$ is likely to err on the high side, the agreement with the value estimated above for the pigeon is remarkably close.

The recent respirometric measurements of Tucker (1968) on the budgerigar (*Melopsittacus undulatus*) provide another estimate of $(L/D)_{eff}$ in a different species, by another method again. At the minimum-power speed (35 km./hr.) the oxygen

consumption of a budgerigar weighing 35 g. wt. was found to be 10·2 ml./min. in excess of resting metabolism. Assuming that 4 J. of mechanical work are done per ml. of oxygen consumed, the power output would be 0·68 W., and the effective lift: drag ratio 4·9 (from equation 26). Similarly, measurements of oxygen consumption at 28, 42 and 48 km./hr. yield estimates for $(L/D)_{eff}$ of 3·8, 4·9 and 4·0 respectively.

Oxygen consumption

If one assumes that 2·03 l. of oxygen are required to oxidize 1 g. of fat (Prosser & Brown, 1961), then the oxygen consumption corresponding to the mechanical power output at the minimum power speed would be 132 ml./min. To this must be added 5 ml./min. for resting metabolism (Lasiewski & Dawson, 1967), making 137 ml./min.

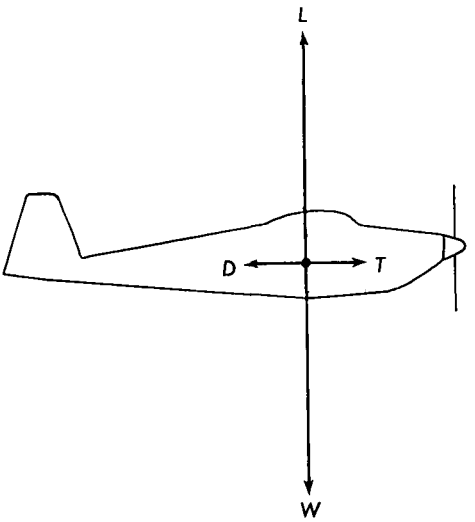

Fig. 14. Equilibrium diagram for level unaccelerated flight in a fixed-wing aeroplane. The weight is balanced by the lift and the drag by the thrust.

in all, as an estimate of the minimum possible oxygen consumption for a pigeon in continuous horizontal flight. At the maximum-range speed the figure would be 168 ml./min. There is little doubt that pigeons can fly continuously at this speed, as Michener & Walcott (1967) record cruising speeds ranging from 13 to 18 m./sec. in different homing pigeons, so the above argument, if correct, implies that pigeons are capable of absorbing oxygen continuously at a rate of 170 ml./min. or so.

There is equally little doubt that pigeons are *not* able to remain in oxygen balance while hovering. They can hover for a few seconds, but presumably rely on the white fibres of the pectoralis to do this (George & Berger, 1966), and incur an oxygen debt.

It follows that the maximum power which a pigeon can produce without incurring an oxygen debt must lie somewhere between that required to cruise at the maximum-range speed and that required to hover, and this defines a *speed range* (with a lower as well as an upper limit) over which continuous flight is possible. For instance, if 16 m./sec. is assumed to be the upper limit, one can draw a horizontal line at about 10·5 W.

in Fig. 12 representing the maximum continuous power output. The pigeon would then be able to fly in oxygen balance at speeds between 3 and 16 m./sec., but would incur an oxygen debt at both lower and higher speeds.

Maximum power

To complete the diagram, one also needs to know the maximum power which the pigeon can achieve in short bursts of activity, for instance at take-off. An estimate of this maximum power can be made from Pennycuick & Parker's (1966) observation that pigeons can climb vertically at 250 cm./sec. when forced to take off close to an obstacle. Five observations of steep or vertical take-off on the high-speed film yielded flapping frequencies ranging from 9·1 to 9·7/sec., averaging 9·4/sec., and the sweep angle was taken to be 284°, the maximum anatomically possible. The power required for vertical climb was then calculated in the same way as was done earlier for horizontal flight.

Profile power worked out to be 5·6 W., and parasite power was 0·05 W. Induced power (4·9 W.) was considerably less than in hovering (8·4 W.), because the vertical climbing velocity increases the mass flow of air through the wing disk, thus reducing the induced velocity needed to maintain the required rate of change of momentum. The *climbing power* (product of weight and vertical velocity) was 9·8 W., and the total power required 20·4 W., or nearly twice the maximum continuous power. In the case of the pigeon it is no surprise to find a large difference between maximum power and maximum continuous power, since the work of J. C. George and co-workers (reviewed by George & Berger, 1966) has shown that a large part of the pigeon's flight muscle is specialized for intermittent anaerobic operation. The ratio of these two powers would, however, be expected to vary widely in different flying animals.

Structural considerations

(*a*) *Air loads*

If the pectoralis applies a moment M to the humerus during the downstroke, and rotates the wing at an angular velocity ω, the total power output (for both wings) is

$$P = 2M\omega.$$

Since all the work is assumed to be done on the downstroke, and none on the upstroke however, the average power is half of this. If P and ω have been calculated, M can be estimated as

$$M = \frac{P}{\omega}. \tag{28}$$

Average values for M at different speeds, calculated from equation (28), are plotted against speed in Fig. 15.

A maximum value for M, averaging 10·2 kg. wt. cm., was found by Pennycuick & Parker (1966) by measuring the ultimate strength of the pectoralis insertion. A minimum value can be obtained by assuming that during the downstroke the wing must support at least half the weight, or 200 g. wt. for a 400 g. wt. pigeon. The position of the centre of lift of the wing in gliding (which would be much the same as in fast

flapping flight) was estimated by Pennycuick (1967) to be 14·3 cm. from the centre of rotation of the shoulder joint, giving a minimum possible moment of 2·9 kg. wt. cm. These upper and lower limits are marked in Fig. 15.

(*b*) *Inertial loads*

It might be thought that the work done in imparting angular kinetic energy to the wing at the beginning of each downstroke and each upstroke should have been considered in the power calculation. This energy is, however, recoverable, since the wing can be slowed by aerodynamic forces at the end of the stroke, and its kinetic energy can, in principle, be transferred to the air. The power needed to oscillate the wing is thus included in induced and profile power, and need not be considered separately—in contrast to the case of a walking mammal, for instance, in which the biggest component of power is that needed to oscillate the legs.

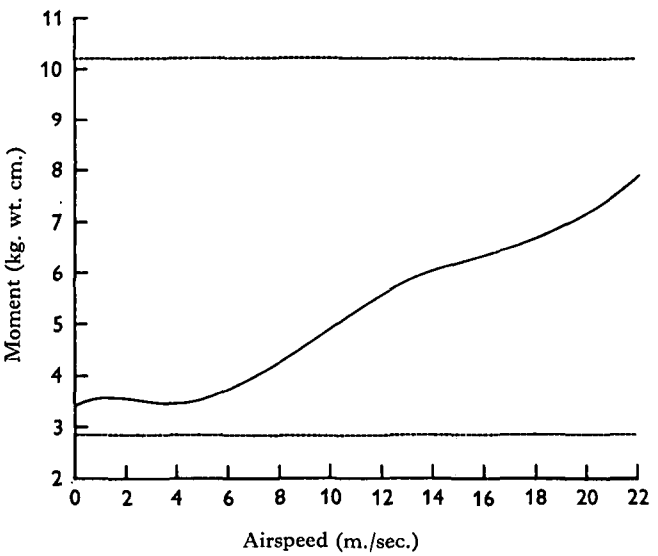

Fig. 15. Calculated average moment exerted by the pectoralis in the downstroke of horizontal flight in the pigeon. The upper horizontal line represents the ultimate moment sufficient to break the pectoralis insertion, and the lower line is the minimum needed to balance the bird's weight.

When the forces applied to the structure are considered, the moments needed to accelerate the wings must be taken into account. In order to obtain some idea of the magnitude of these moments, the moment of inertia of a pigeon's wing was estimated as follows.

A wing was removed at the shoulder joint from a pigeon which had been killed the previous day, frozen, and partially thawed: it was set up in the fully extended position, and re-frozen. It was then cut into sixteen strips, by chordwise cuts made with a photographic guillotine, and each strip was weighed. The spanwise distance between successive cuts was 2 cm., and the centres of mass of the strips were taken to be 1, 3,

5, etc., cm. from the centre of rotation of the shoulder joint. The moment of inertia I of the wing was calculated from the formula

$$I = \sum_{i=1}^{i=16} r_i^2 m_i, \tag{29}$$

where r_i, m_i are the flapping radius and mass respectively of strip i. The mass of the wing was 24·3 g., and its moment of inertia was estimated as 1830 g. cm.^{2}.

The greatest inertial loads would presumably occur in vertical climbing, where both sweep angle and flapping frequency are maximal. If it is assumed that the wing sweeps through its full travel (142° for one wing) in half a cycle, then at a flapping

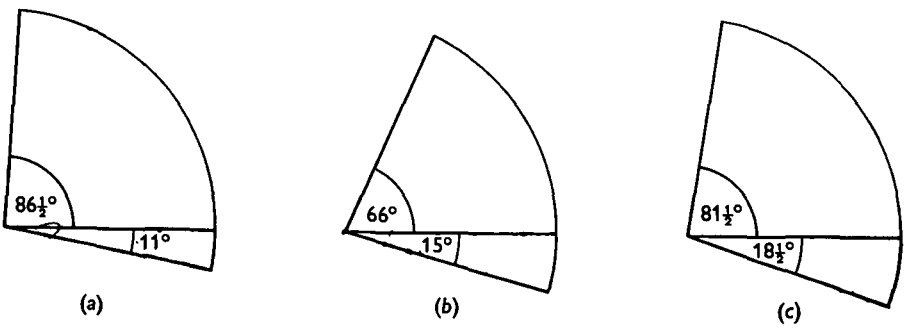

Fig. 16. Average travel of the wing above and below horizontal, in a pigeon flying horizontally at different speeds. (*a*) Speed 7·8 m./sec., flapping frequency 6·20/sec. (*b*) 9·2 m./sec., 6·00/sec. (*c*) 18·0 m./sec., 5·57/sec.

frequency of 9·4/sec. the average angular velocity would be 47 radians/sec. As the whole downstroke would last 53 msec., one could hardly assign more than 15 msec. for acceleration of the wing, giving an angular acceleration $\dot{\omega}$ of at least $3{\cdot}1 \times 10^3$ radians/sec.^{2}. The moment M required to produce this is

$$M = I\dot{\omega} = 5{\cdot}7 \times 10^6 \text{ dyne cm.} = 5{\cdot}8 \text{ kg. wt. cm.}$$

The moment due to air loads in vertical climbing is estimated as 4·5 kg. wt. cm., so that if the ultimate moment which the pectoralis can carry is 10·2 kg. wt. cm., it would seem that the pectoralis could support either the air loads in vertical climbing or the inertial loads, but not both simultaneously. It seems most likely that the wing is first accelerated from the fully 'up' position at low or zero angle of attack, so that the air loads are initially small, and that once the angular velocity has reached its full value, the angle of attack is increased, and the air loads are allowed to develop.

This idea is supported by the fact that the wings are always raised farther above the horizontal position on the upstroke than they are depressed below it on the downstroke—in maximal flapping the wings are clapped togtether above the back, but the humeri are only depressed some 45° below the mid-point on the downstroke. The point is illustrated in Fig. 16, which is derived from the experiment described on page 528, and shows the average angular excursion of the wing in horizontal flight at various speeds. There would seem little aerodynamical advantage in raising the wings farther than they are lowered, and probably the early part of the downstroke is used mainly or solely for accelerating the wing.

Structural safety factor

The ratio of the ultimate moment, sufficient to break the pectoralis insertion, to the maximum moment likely to be developed in flight may be defined as the 'structural safety factor' of the pectoralis insertion. It is estimated as 1·6 at the maximum range speed, and 2·3 in vertical climbing. This may be compared with Machin & Pringle's (1959) estimate that the tensile stress needed to tear the flight muscles of the beetle *Oryctes rhinoceros* is about 1·9 times the maximum stress developed in flight.

DISCUSSION

Variation of the power curve

The general U-shape of the power-versus-speed curve of Fig. 12 probably applies to all flying animals, but the high-power portions at the two ends are caused by different factors, and are to some extent independent. The high power needed in hovering and at low speeds is due to the induced component, which can be reduced by reducing the disk loading. Thus animals specialized for hovering can economize on induced power (at the expense of high-speed performance) by evolving long wings, which may be the explanation of Greenewalt's (1962) observation that the larger hummingbirds have disproportionately long wings as compared to the smaller ones.

The rise in the power curve at high speeds, on the other hand, is mainly due to the drag of the body, though wing-profile power ($P_{\text{pro}\,2}$) also contributes to it: it can be delayed to some extent by better streamlining of the body, and also by reduction of wing area.

In an attempt to make a comparison with an entirely different bird, a power curve was calculated for the ruby-throated hummingbird *Archilochus colubris*, by the same method as was used for the pigeon. The data required in the computer program were obtained from figures and drawings given by Greenewalt (1961, 1962), and are listed in the appendix. The results are plotted in Fig. 17. The maximum power line has been drawn to give the maximum level speed of 11·5 m./sec., recorded by Greenewalt (1961) for this species, and the maximum continuous power must lie between this and the hovering power (p. 550).

The best effective lift:drag ratio is estimated to be only 4·1 for this bird, but this corresponds to a range of 894 km./g. fat, achieved at 9 m./sec. (20 m.p.h.). If, as Lasiewski (1962) says, the bird can carry 2 g. of fat, it should be able to cross the Gulf of Mexico with a large safety margin, and the trip would take 25 hr. in no wind. The low speed at which maximum range is obtained, however, means that a headwind of only 4·5 m./sec. (10 m.p.h.) would double the time for the crossing and use up the fuel reserve, and from this point of view a long sea crossing is safer for a large bird which can cruise at a higher speed. As explained on page 541, the larger bird has no advantage in air range as such, by virtue of its size. The implications of the present study for the theory of bird migration are developed further by Pennycuick (1969).

Lift coefficient

The maximum estimated value of lift coefficient for the pigeon is 2·78 and occurs in hovering. The maximum value of 2·15 calculated for the ruby-throated humming-

bird occurs at 1·5 m./sec., and is somewhat higher than the hovering value (1·86). The general similarity of the range of estimated lift coefficients in the two species can be seen from Fig. 18.

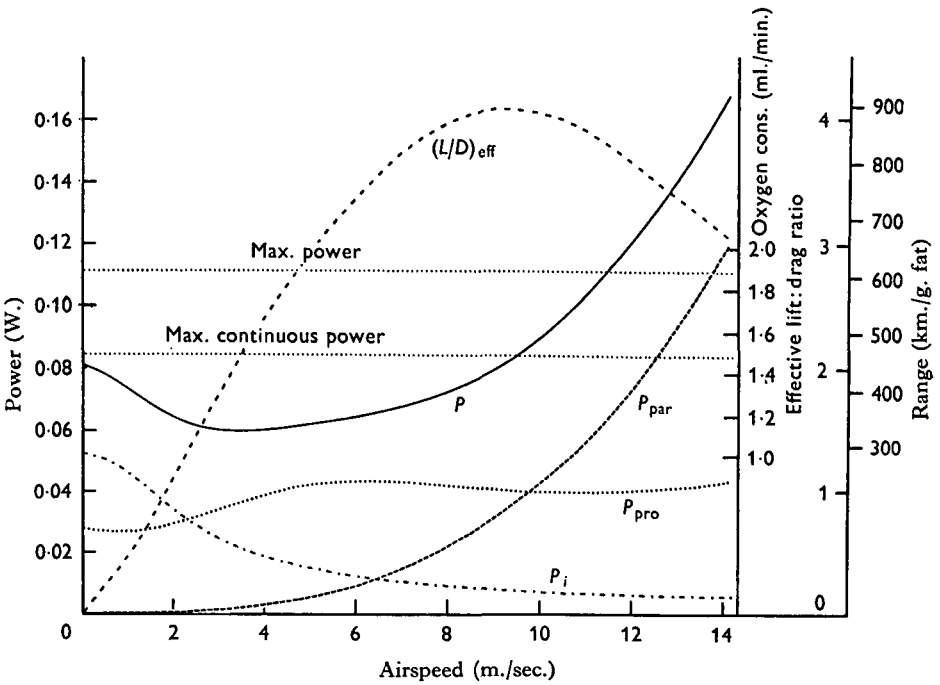

Fig. 17. Power calculation as Fig. 12, for the ruby-throated hummingbird *Archilochus colubris*. The calculation is based on data listed in the appendix, and derived from Greenewalt (1961, 1962). P_i, Induced power; P_{pro}, profile power; P_{par}, parasite power; P, total power (power scale at left, corresponding oxygen consumption scale at right). $(L/D)_{eff}$, effective lift:drag ratio (scale at far right, with corresponding range scale).

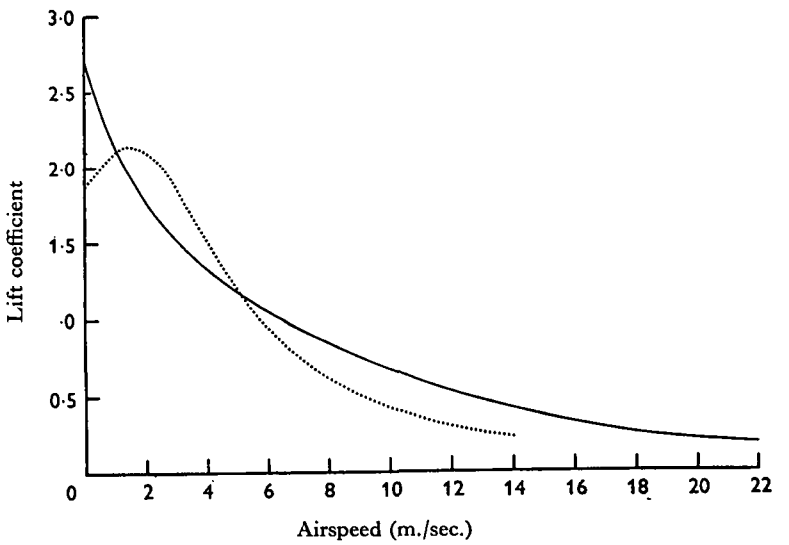

Fig. 18. Calculated lift coefficient in horizontal flight for the pigeon (solid line) and ruby-throated hummingbird (dotted line), plotted against forward speed.

Application to animals of different size

Although the general U-shape of the power curve of Figs. 12 and 17 is likely to apply to all flying animals (as it does to helicopters), one would expect the relationships of the maximum, and maximum continuous, power levels to the curve to vary in a systematic way in animals of different size. The power required to fly and the power available from the muscles vary in different ways with the size of the animal, and the nature of the general trend can be deduced from a simple dimensional argument.

Effect of size on power required

In geometrically similar animals the weight W is proportional to the cube of any representative length, which can be expressed by the proportionality

$$W \propto l^3. \tag{30}$$

Similarly, any surface area, such as the wing-area S, is proportional to length squared:

$$S \propto l^2. \tag{31}$$

Greenewalt's (1962) fig. 3 shows that these relations are broadly obeyed throughout the entire range of flying animals ('gnat to condor'), and although there is some scatter, very large departures from the general trend are mechanically impracticable. It is broadly true that in flying animals of different size the wing-loading, W/S, is proportional to length, since

$$\frac{W}{S} \propto \frac{l^3}{l^2} = l. \tag{32}$$

Now any representative speed V on the curve of Fig. 12, such as the minimum-power speed or the maximum-range speed, will normally occur at a particular lift coefficient, and will therefore vary in proportion to the square root of the wing-loading:

$$V \propto \sqrt{\left(\frac{W}{S}\right)} \propto l^{\frac{1}{2}}. \tag{33}$$

Referring to the simple representation of powered flight shown in Fig. 14, and assuming a constant lift:drag ratio, the thrust T required is proportional to the weight:

$$T \propto W \propto l^3 \tag{34}$$

and the power required P_r is

$$P_r = TV \propto l^3 \times l^{\frac{1}{2}} = l^{3\cdot5} \propto W^{\frac{7}{6}}. \tag{35}$$

The power required for any particular state of flight increases approximately with the 1·17 power of the weight, because larger animals in general have higher wing-loadings, and are therefore obliged to fly faster. This argument is well known in aeronautics, and is given in connexion with birds by Wilkie (1959).

Effect of size on power available

Greenewalt (1962) found that the mass of the pectoralis plus supracoracoideus muscles is about 17% of the body weight in birds of any size (except in hummingbirds, which have relatively more flight muscle), so the mass of the flight muscles

may be taken as proportional to the body weight. The work done, Q, per contraction by a muscle of given type is proportional to the mass of the muscle, regardless of its shape (Hill, 1950).

$$Q \propto l^3. \tag{36}$$

The contraction frequency F is inversely proportional to length—large animals are obliged to oscillate their limbs at a lower frequency than small ones, for the structural reasons given by Hill (1950).

$$F \propto l^{-1}. \tag{37}$$

The power output P_a is the product of the work done per contraction and the contraction frequency, so that

$$P_a = QF \propto l^2. \tag{38}$$

At this level of argument the power available P_a is considered in a general way without making the distinction explained on page 553 between maximum power available and maximum power continuously available. As in non-flying animals, P_a is more nearly proportional to surface area than to mass or volume.

If the logarithms of P_a and P_r are plotted against the logarithm of the weight for flying animals of different size, the slope of the former line should be 2/3, and that of the latter 7/6 (Fig. 19). Even allowing for the rather vague nature of the above argument, the difference between these two slopes is so large that there is bound to be a sharp upper limit to the size of practicable flying animals. In practice the limit of mass for flying birds seems to be in the region of 12 kg. (with the crop empty), and is attained by some species of at laest three different orders—examples are the Kori bustard *Ardeotis kori*, the California condor *Gymnogyps californianus* and the trumpeter swan *Cygnus cygnus*.

General performance limitations

Figure 20 illustrates the way in which the differing relationship of the maximum power available, P_{am}, and the maximum power continuously available, P_{ac}, to the power required, P_r, determines the general flight capabilities of four different-sized birds.

In the case of hummingbirds (Trochilidae), whose mass ranges from 2 to 20 g., it seems that sufficient power is available for hovering without incurring an oxygen debt—Lasiewski (1963) records a specimen of *Calypte costae* hovering continuously for 50 min. The P_{ac} line may therefore be drawn in above the hovering power (Fig. 20*b*), and the P_{am} line somewhat higher. The pigeon *Columba livia* (mass 400 g.) is an intermediate case in that the P_{ac} line falls between the minimum power required (trough of curve) and the hovering power, whereas P_{am} is well above the hovering power. The pigeon is thus able to jump straight into the air on take-off and can climb vertically for perhaps a second if necessary, but it cannot fly continuously more slowly than about 3 m./sec. (Fig. 20*a*).

Turning now to very large birds, the larger African vultures (mass 5–7 kg.), such as the lappet-faced vulture *Torgos tracheliotus* and the white-backed vulture *Pseudogyps africanus*, cannot hover even briefly, but they can fly horizontally for short periods, possibly for 5 min. Thus both P_{am} and P_{ac} must lie between the minimum power required and the hovering power (Fig. 20*c*). It would appear from the account of Koford (1953) that the even larger California condor (mass up to 12 kg.) is probably not capable of continuous horizontal flight at all, and relies exclusively on soaring for

protracted flight, flapping its wings only on take-off or in emergencies. If this is so, its P_{am} would lie above the trough of the power required curve, but P_{ac} would lie below it (Fig. 20*d*).

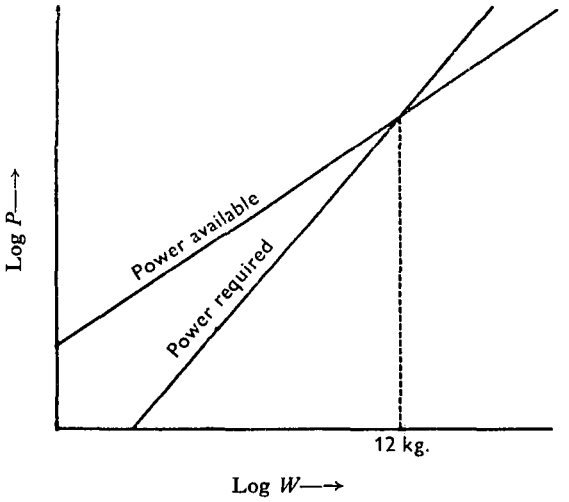

Fig. 19. Double logarithmic plot of power required (P_r) and power available (P_a) against weight for geometrically similar flying animals of different size.

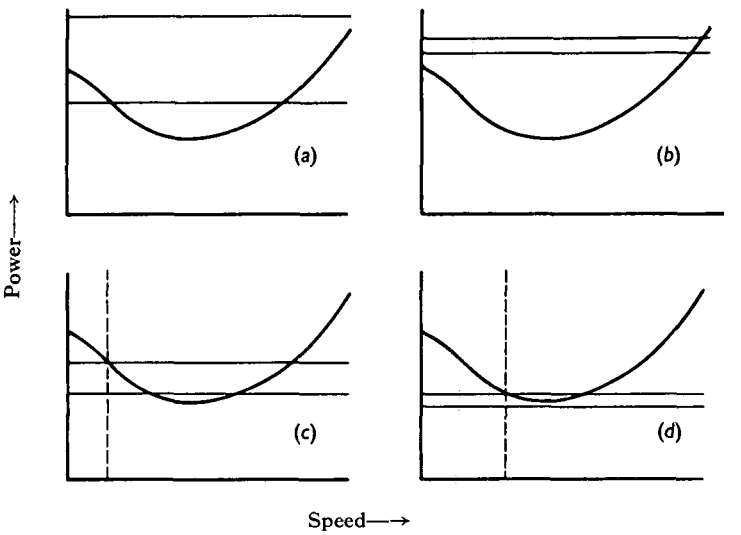

Fig. 20. Power curves as in Fig. 12 and Fig. 17 for (*a*) pigeon, (*b*) hummingbird, (*c*) white-backed vulture, and (*d*) California condor (not to scale). The upper horizontal line represents maximum power available, the lower one maximum power continuously available. The vertical dotted lines in (*c*) and (*d*) represent take-off speed.

Take-off

It follows from diagrams of the type shown in Fig. 20*c*, *d* that large birds cannot jump into the air from flat ground like a pigeon, but must accelerate horizontally to a speed V_{min}, marked by the vertical dotted lines, at which they have sufficient power to

maintain horizontal flight. If the bird takes off against a wind blowing at V_{min} or faster, it can, of course, become airborne at once, but in still air, on flat ground, V_{min} must be attained by running.

The heavier the bird, and the higher its wing-loading, the greater is V_{min}. Maximum running speed, however, does not increase noticeably with increasing size, and Hill (1950) showed that for geometrically similar animals running speed should be independent of size. Thus there must be a size of bird whose maximum running speed would be insufficient to accelerate it to V_{min}, and which could not, therefore, take off in no wind from flat ground, and it is possible that this factor places an upper limit on the size and/or wing-loading of large flying birds which inhabit flat country. An alternative method of taking off, which is normally available to mountain birds like the California condor, is to jump off some eminence, which avoids the need for a take-off run. It may be noted that birds are the only flying vertebrates which have ever been able to take off by running over the ground; in both bats and pterosaurs the legs are (or were) modified as part of the wing structure, and thereby rendered unsuitable for bipedal running. The larger members of these groups could therefore only take off by diving from a tree or hill.

General performance standards

The general level of performance measured or deduced for the pigeon is extremely poor by aeronautical engineering standards. Wing-profile drag coefficients ranging from 0·01 to 0·54 are deplorably high, as is the body-drag coefficient of 0·43, and the resulting estimate of about 6 for the best effective lift: drag ratio is far from impressive. However, these figures lead to entirely plausible estimates of the pigeon's general flight capabilities, and there is no reason at present to doubt that its performance is indeed as poor as has been suggested. This is strongly supported by the very similar estimates of effective lift: drag ratio deduced from the measurements of Nisbet *et al.* (1963) and Tucker (1968), using different species and radically different methods (p. 542). The above calculation for the ruby-throated hummingbird confirms the same general impression.

The performance of model aircraft, operating in the same range of Reynolds numbers (20,000–300,000) as the birds mentioned here, is also very poor by comparison with that of full-scale aircraft. The latter mostly operate at Reynolds numbers of 1 million upwards, at which it is usually possible to keep the boundary layer laminar over a substantial fraction of the wing surface. Following the advice of Schmitz (1960), who investigated the behaviour of a number of aerofoil sections at low Reynolds numbers, aeromodellers commonly glue sandpaper or thread along the leading edge of their models' wings, which ensures that the boundary layer is turbulent all over, since only in this case (at low Reynolds numbers) will the boundary layer remain attached to the wing surface over a useful range of angles of attack. The performance estimates for birds given here are consistent with the idea that they, too, maintain a fully turbulent boundary layer over the whole wing at all times, doubtless for the same reason.

SUMMARY

1. Certain measurements made on pigeons flying horizontally in a wind-tunnel are described.

2. A method, based on helicopter theory, for calculating the power required to fly at any given speed is explained. Induced, profile and parasite power are calculated separately.

3. It is concluded that the pigeon can fly horizontally without incurring an oxygen debt at speeds from 3 to 16 m./sec. The minimum power speed is 8–9 m./sec. The maximum continuous power output is estimated to be 10·5 W., and the corresponding oxygen consumption about 170 ml./min. The maximum (sprint) power is estimated to be 20·4 W., from observations of vertical climb after take-off.

4. The estimated best lift:drag ratio in horizontal flight is 5·9, giving a range of 11·8 km./g. of fat oxidized for a 400 g. pigeon.

5. It is argued from considerations of structural strength that the early part of the downstroke is used mainly to impart angular velocity to the wing, and that air loads are only developed after most of the angular acceleration has taken place. The tension in the pectoralis insertion may exceed 60% of the breaking tension in fast horizontal flight.

6. The power calculation was repeated for the ruby-throated hummingbird, using published data. Estimated best range is about 900 km./g. of fat oxidized, achieved at 9 m./sec. The corresponding effective lift:drag ratio is 4·1.

7. The variation of power required and power available with size is considered, and the effect on hovering and take-off performance of different birds deduced.

8. Performance estimates for the pigeon and ruby-throated hummingbird are very poor by engineering standards, but consistent with these birds' known abilities, and are in general agreement with estimates of effective lift:drag ratio derived from published data on other species.

In addition to those to whom my thanks are acknowledged in the preceding paper, I am most grateful to Dr L. C. Strong for carrying out the Soxhlet extraction mentioned on page 541.

REFERENCES

BROWN, R. H. J. (1948). The flight of birds: the flapping cycle of the pigeon. *J. exp. Biol.* **25**, 322–33.

GEORGE, J. C. & BERGER, A. J. (1966). *Avian Myology*. New York: Academic Press.

GREENEWALT, C. H. (1961). *Hummingbirds*. New York: Doubleday.

GREENEWALT, C. H. (1962). Dimensional relationships for flying animals. *Smithsonian misc. Coll.* **144**, no. 2.

HILL, A. V. (1950). The dimensions of animals and their muscular dynamics. *Science Progr.* **38**, 209–30.

KOFORD, C. B. (1953). *The California Condor*. New York: Dover.

LASIEWSKI, R. C. (1962). The energetics of migrating hummingbirds. *Condor* **64**, 324.

LASIEWSKI, R. C. (1963). Oxygen consumption of torpid, resting, active and flying hummingbirds. *Physiol. Zool.* **36**, 122–40.

LASIEWSKI, R. C. & DAWSON, W. R. (1967). A re-examination of the relation between standard metabolic rate and body weight in birds. *Condor* **69**, 13–23.

MACHIN, K. E. & PRINGLE, J. W. S. (1959). The physiology of insect fibrillar muscle. II. Mechanical properties of a beetle flight muscle. *Proc. R. Soc.* B **151**, 204–25.

MICHENER, M. C. & WALCOTT, C. (1967). Homing of single pigeons—analysis of tracks. *J. exp. Biol.* **47**, 99–131.

NISBET, I. C. T., DRURY, W. H. & BAIRD, J. (1963). Weight loss during migration. I. Deposition and consumption of fat by the blackpoll warbler *Dendroica striata*. *Bird Banding* **34**, 107–38.

PENNYCUICK, C. J. (1967). The strength of the pigeon's wing bones in relation to their function. *J. exp. Biol.* **46**, 219–33.

PENNYCUICK, C. J. (1968). A wind-tunnel study of gliding flight in the pigeon *Columba livia*. *J. exp. Biol.* **49**, 509–26.

PENNYCUICK, C. J. (1969). The mechanics of bird migration. *Ibis* (in press).

PENNYCUICK, C. J. & PARKER, G. A. (1966). Structural limitations on the power output of the pigeon's flight muscles. *J. exp. Biol.* **45**, 489–98.

PROSSER, C. L. & BROWN, F. A. (1961). *Comparative Animal Physiology*. Philadelphia: Saunders.

SCHMITZ, F. W. (1960). *Aerodynamik des Flugmodells*. Duisberg: Lange.

SHAPIRO, J. (1955). *Principles of Helicopter Engineering*. London: Temple Press.

TUCKER, V. A. (1968). Respiratory exchange and evaporative water loss in the flying budgerigar. *J. exp. Biol.* **48**, 67–87.

WILKIE, D. R. (1959). The work output of animals: flight by birds and by man-power. *Nature, Lond.* **183**, 1515–16.

APPENDIX

The following data were used in the power calculations for the pigeon and ruby-throated hummingbird.

	Columba livia	*Archilochus colubris*
Weight (g. wt.)	400	3·7
Disk area (cm.^{2})	3500	72
Air density (g. cm.$^{-3}$)	$1{\cdot}22 \times 10^{-3}$	$1{\cdot}22 \times 10^{-3}$
Flapping frequency (sec.$^{-1}$)	See Fig. 4	52
Inclination of flapping plane (degrees)	See Fig. 6	0 in hovering 57 at 3·84 m./sec. 78 at 11·6 m./sec.
Sweep angle (degrees)	See Fig. 3	233 in hovering 131 at 3·84 m./sec. 160 at 11·6 m./sec.
Body frontal area (cm.^{2})	36	1·6
Body drag coefficient	0·43	0·43
Wing profile drag coefficient	See Fig. 11	See Fig. 11

Wing strip areas and flapping radii

Columba livia			*Archilochus colubris*		
Strip	Area (cm.^{2})	Flapping radius (cm.)	Strip	Area (cm.^{2})	Flapping radius (cm.)
1	12·0	1	1	0	0·11
2	12·6	2	2	0·23	0·33
3	12·8	3	3	0·31	0·55
4	12·8	4	4	0·32	0·76
5	12·8	5	5	0·32	0·98
6	12·8	6	6	0·33	1·20
7	12·8	7	7	0·33	1·42
8	13·0	8	8	0·32	1·63
9	13·3	9	9	0·32	1·85
10	13·4	10	10	0·32	2·07
11	13·3	11	11	0·31	2·29
12	13·2	12	12	0·31	2·51
13	12·9	13	13	0·30	2·73
14	13·3	14	14	0·29	2·94
15	13·5	15	15	0·27	3·16
16	13·1	16	16	0·26	3·38
17	13·0	17	17	0·25	3·60
18	12·2	18	18	0·24	3·81
19	12·4	19	19	0·23	4·03
20	12·0	20	20	0·19	4·25
21	11·5	21	21	0·12	4·47
22	11·4	22	22	0·06	4·69
23	10·6	23			
24	10·5	24			
25	9·5	25			
26	9·1	26			
27	7·8	27			
28	7·2	28			
29	6·1	29			
30	4·6	30			
31	3·7	31			
32	2·4	32			